Available online at www.sciencedirect.com

ScienceDirect

Geochimica et Cosmochimica Acta 137 (2014) 134–146

Geochimica et Cosmochimica Acta

www.elsevier.com/locate/gca

Smouldering fire signatures in peat and their implications for palaeoenvironmental reconstructions

Claudio Zaccone [a,b,*], Guillermo Rein [c], Valeria D'Orazio [d], Rory M. Hadden [c,e], Claire M. Belcher [f], Teodoro M. Miano [d]

[a] Department of the Sciences of Agriculture, Food and Environment, University of Foggia, via Napoli 25, 71122 Foggia, Italy
[b] Department of Renewable Resources, University of Alberta, 348E South Academic Building, T6G 2H1 Edmonton, Canada
[c] Department of Mechanical Engineering, Imperial College London, London SW7 2AZ, UK
[d] Department of Soil, Plant and Food Sciences, University of Bari "Aldo Moro", via Amendola 165/A, 70126 Bari, Italy
[e] School of Engineering, University of Edinburgh, Edinburgh EH9 3JL, UK
[f] Department of Geography, University of Exeter, Exeter EX4 4PS, UK

Received 13 August 2013; accepted in revised form 13 April 2014; available online 24 April 2014

Abstract

Peatland ecosystems are valued as natural archives of past climatic and vegetation changes and as such their study is essential for palaeoenvironmental reconstructions over millennia. Fires in peatlands are dominated by smouldering combustion which is the self-sustained, slow, low temperature, flameless form of burning. Most studies on peat fires to date have focused on ignition conditions, C losses or atmospheric emissions, but there is a significant gap in the understanding of the evolution of organic matter (OM) following smouldering. A key feature of smouldering fires is that they consume most of the pyrogenic char produced. Consequently, it may be that most smouldering fires are simply not visible using standard palaeontological techniques. Here we present the possibility of identifying palaeofires by following their physical and chemical signature along a peat profile. We have undertaken laboratory experiments on *Sphagnum* peat columns and measured physical, chemical and spectroscopic changes of OM features induced by smouldering on samples of varying moisture content. We reveal that there is a higher production of aromatic and condensed molecules, an increase of the total N and a decrease of the C/N ratio, besides significant variations of pH, electrical conductivity and ash content. Several of these changes have, in previous studies, been taken to be indicative of alterations in atmospheric dust deposition and climate-driven changes (e.g., vegetation, water table fluctuation, decomposition and mineralization processes), but are also produced by smouldering fires. Our results imply that smouldering fires should therefore also be considered in climatic and floral reconstructions drawn from peat cores and that these additional physical and chemical changes may serve to enhance our understanding of palaeofire histories.

1. INTRODUCTION

The burning of soil organic matter (SOM) during wildfires has affected Earth's terrestrial ecosystems for hundreds of millennia; however, the influence of wildfire events on the fate of SOM is still not completely understood. Studies of chemical changes on a range of soil types following wildfires mostly concentrate on erosion, ash, nutrient availability, microbial dynamics and plant species recovery

* Corresponding author at: Department of the Sciences of Agriculture, Food and Environment, University of Foggia, via Napoli 25, 71122 Foggia, Italy. Tel.: +39 0881589119.
E-mail address: claudio.zaccone@unifg.it (C. Zaccone).
URL: http://www.claudiozaccone.net (C. Zaccone).

http://dx.doi.org/10.1016/j.gca.2014.04.018
0016-7037/

(e.g., Viro, 1974; Raison, 1979; Giovannini et al., 1987, 1990; Pyne, 2001; Smith et al., 2001, 2008; Villar et al., 2004; Certini, 2005; Beck et al., 2011), whereas only few works focus on changes of SOM features (e.g., González-Pérez et al., 2004; Knicker et al., 2005, 2008; Knicker, 2010; Alexis et al., 2012).

The SOM-rich ecosystems which are most affected by fire are peatlands. Peat is particularly flammable in dry conditions and when it burns, the dominating phenomenon is not flaming but rather smouldering combustion (Rein, 2013). Smouldering is the slow, low temperature, flameless form of combustion of organic matter (OM) in porous form (Ohlemiller, 1985), and represents the most persistent type of combustion phenomena (Rein, 2013). Smouldering megafires in peat deposits occur frequently during the dry season in tropical, temperate and boreal ecosystems, e.g., South-East Asia, Northern America, British Isles, Southern Africa and others. Once ignited, these fires are particularly difficult to extinguish despite extensive rainfalls, weather changes, or fire-fighting attempts. This means that these fires can persist for long periods of time (months or years) providing the fire with time to spread deep into the ground and over large areas.

No global studies exist on the frequency of peat fires in literature. The most studied peat megafire occurred in Indonesia during 1997 and led to an extreme smoke haze event. These fires are estimated to have released the equivalent of 13–40% the mean annual global C emissions from fossil fuels (Page et al., 2002). The 1997 megafire was not an isolated case in the region; such haze episodes have drifted to South East Asia once every three years on average (Field et al., 2009). Rough figures at the global scale suggest that mean annual greenhouse gas emissions from smouldering peat fires are equivalent to >15% of anthropogenic emissions (Poulter et al., 2006). Consequently, smouldering fires represent a large perturbation within peatlands and to atmospheric chemistry. Moreover, it is anticipated that the release of ancient C during peat fires creates a positive feedback mechanism in the climate system, i.e., a self-accelerating process that would lead to more smouldering fires (Rein, 2013). Warmer temperatures at high latitudes are already resulting in unprecedented permafrost thaw (Tarnocai et al., 2009), leaving large organic C pools exposed to fires for the first time in millennia.

The smouldering process is driven by the heat released from heterogeneous oxidation of porous fuel as it reacts with the oxygen in the atmosphere (Ohlemiller, 1985). Smouldering chemistry can be approximated by a two-step process: the pyrolysis of the OM produces pyrogenic char which is then oxidized *in situ* (Hadden et al., 2013; Rein, 2013). This means that whilst smouldering fire creates char, it also consumes it, a factor little considered in palaeofire reconstructions.

Given its persistence and presence in a wide range of modern ecosystems, it can be argued that smouldering played an important role in Earth's ancient ecosystems. Much of our knowledge of past fire events is based on the abundance of charcoal particles in the fossil and subfossil records (e.g., Scott, 2010; Mooney and Tinner, 2011). The combustion of char by the smouldering process implies that the record of past fires in peat cores may be entirely hidden using standard techniques that quantify charcoal in palynology or mesofossil preparations (e.g., Scott, 2010; Mooney and Tinner, 2011). We may therefore be missing important information about variations in fire frequency in peat soils (and in bogs, in particular) which are seen as essential for palaeoenvironmental reconstruction because they serve as natural archives of climatic and vegetation changes occurring during the past millennia (e.g., Aaby, 1976; van Geel, 1978; Shotyk et al., 2002; Tareq et al., 2004; Zaccone et al., 2011a; Langdon et al., 2012).

Through a laboratory study, we seek to address this bias in *Sphagnum* peat records trying to identify palaeofires by the physical, chemical and spectroscopic signature that they leave behind in the soil profile. It is also hoped to provide a new "key of reading" of some physical and chemical signatures previously ascribed exclusively to "traditional" climate-driven changes.

2. MATERIALS AND METHODS

2.1. Preparation of peat columns

We have created three laboratory mesocosms, each of them made of pure *Sphagnum* peat moss from a commercially available source which provides a consistent, repeatable and homogenous source of samples. The choice to conduct our study on "constructed" samples rather than on natural peat cores was imposed by the need to distinguish between changes caused by the smouldering fire and those that occur due to the heterogeneity of peat samples along a profile.

After drying and water addition to reach the desired moisture content (MC) value, samples were thoroughly mixed before each experiment. The peat column height was kept constant for all tests. Ignition was applied on top of the core (Fig. 1a) and the fire is allowed to spread downwards (Fig. 1b).

The column set up was chosen in order to observe how the fires interact at depth and to best capture the post-fire physical and chemical gradients in the vertical direction. The majority of previous experiments of smouldering peat used shallow horizontal beds (Frandsen, 1997; Rein et al., 2008; Belcher et al., 2010) which are reduced to a thin layer of char and ash after smouldering, and do not provide suitable vertical gradients to study. Our experiments differ from the few previous column experiments (e.g., Benscoter et al., 2011; Watts, 2013) in that our samples are of homogenous composition, thus offering a better control of the fuel features as well as a high repeatability.

The effect of the MC has been considered here in order to reflect the fire behaviour on a peat soil under different conditions. Moisture content, in fact, is the most important property governing the ignition and spread of smouldering fires (Frandsen, 1987; Rein et al., 2008). The prominent role of moisture is such that natural or anthropogenic-induced droughts are the leading cause of peat megafires, i.e., fires showing a fuel consumption per unit area about 100 time larger than in flaming fires (Rein, 2013).

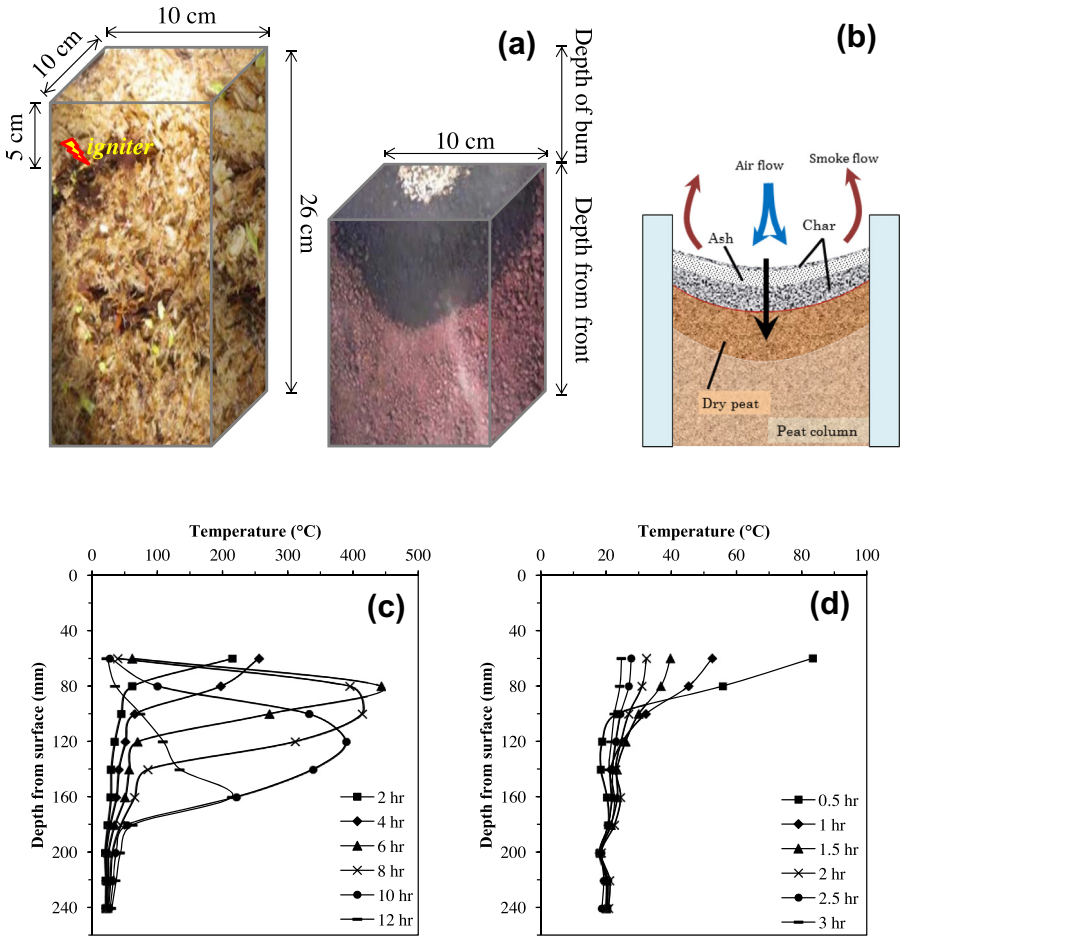

Fig. 1. The smouldering test. In panel (a), a schematic representation of the laboratory peat column before and following the smouldering experiment is shown. The depth from the front represents the vertical distance into the residue starting from the final position reached by the free surface after the smouldering front stopped spreading. Panel (b) shows a diagram of downward propagation in a column of peat (by X. Huang, CC BY license). Panel (c) and (d) show sets of temperature measurements taken at different depths of the columns *vs.* time for 100% and 200% MC series. Peak temperatures reached were 441.9 and 83.2 °C, respectively.

In order to obtain different MC levels, samples were prepared by first drying a batch of the peat at 80 °C, for 48 h, to remove moisture. Peat samples were then mixed with appropriate amounts of water to reach the desired range of MC. Being the column height kept constant for all tests, the dry density of the bulk peat (g $_{dry\ peat}$ cm^{-3}) changed according to the water content; in fact, in natural conditions, a negative correlation was observed between these two parameters (Klemetti and Keys, 1983; Zaccone et al., 2009; Poto et al., 2013). The wet peat was then placed into an airtight container and left to homogenize for one week. The nominal MC values originally desired were 50%, 100% and 200% (in dry weight basis, d.w.; i.e., g $_{water}$/100 g $_{dry\ peat}$), but the actual values reached were 56%, 90% and 211%. These moisture values correspond, in wet weight basis (i.e., g $_{water}$/100 g $_{wet\ peat}$), to 36%, 48% and 68%, respectively, that, in turn, might mirror a peatland under very dry, dry and damp conditions, respectively. Values of MC below the critical threshold [i.e., ~125% MC for a peat showing a mineral content of 8%, according to Frandsen (1997) and Rein et al. (2008)] are not frequent at the local scale in natural wet ecosystems, but at the global level, peatlands are known to reach MC below this value (and significantly lower) under drought or perturbed conditions (e.g., Moreno et al., 2011).

2.2. Smouldering tests

Experiments were conducted on a 26 cm deep column with a 10 × 10 cm square cross section (Fig. 1a). The top surface remained exposed to the atmosphere while the sides and the bottom were insulated from heat losses and air ingress with 2 cm thick plaster board walls and sealed edges. Ignition is attempted using an electrically heated coil buried 5 cm from the top free surface and providing 100 W of energy for a period of 30 min. This is the same ignition protocol used in previous smouldering experiments (Rein et al., 2008; Belcher et al., 2010). Temperatures along the central axis of the column were recorded using 10 K-type thermocouples inserted at 2 cm intervals starting at the bottom of the apparatus.

When power is supplied to the coil, the thermocouple placed closest to the igniter is the first to register heating and the temperature rises until the igniter is turned off 30 min later. A successful peat ignition is followed by sustained smouldering, evidenced by the horizontal and vertical travelling of the peak temperature far from the ignition source (Fig. 1b). Typical peak temperatures of around 450 °C are reached (Fig. 1c). Any arbitrary location of the peat profile sees the successive arrival of four distinct thermal and chemical waves that form the structure of a smouldering front (Rein, 2013). The sample first experiences preheating and is then followed by evaporation of water, pyrolysis of the peat and finally oxidation of the char. The preheating, drying and pyrolysis fronts are sinks of thermal energy and move ahead of the oxidization front where the heat is released and ash is produced. Previous studies show that the residue of a smouldering fire is a combination of ash, char and peat (Hadden et al., 2013) that arranges in horizontal layers and lead to a gradient of composition that depends on the depth from the front. Fig. 1(a, b) includes a visual schematic of this layer structure.

A failed peat ignition (e.g., because of the high MC) is characterized by a drop of the thermocouple readings near the igniter shortly after the ignition source is turned off. In these no-ignition cases, the maximum temperature reached away from the igniter region does not exceed 100 °C (Fig. 1d). After each experiment, the remaining material was collected in 1-cm *ca.* horizontal layers and analyzed.

2.3. Characterization of peat samples

2.3.1. Ash content

The ash content, expressed as a percentage of the original dry weight, was determined for each peat sample by combustion in a muffle furnace at 550 °C for 12 h. All samples were analyzed in triplicate. During the experiments, it was observed that the ash layer results from the accumulation of the combustion residues from the upper column positions.

2.3.2. pH and EC

The pH and the electrical conductivity (EC) were determined on unfiltered samples using a Philips pH-meter equipped with a Hanna Instruments HI 1230 probe and a XS Cond 510 conductimeter, respectively. In both cases, the solid:Milli-Q water ratio (1:20 w:v) was determined considering the dry mass of peat. All samples were analyzed in triplicate.

2.3.3. Elemental composition

Total C, H, N and S concentrations in peat samples were determined in triplicate, using dry combustion with an elemental analyzer (Fisons EA1108, Milan, Italy). The instrument was calibrated by BBOT [2,5-Bis-(5-*tert*-butyl-benzoxazol-2-yl)-thiophen] standard (ThermoQuest Italia s.p.a.). Total organic C was determined by difference between total C and inorganic C (TOC = TC–IC), the latter one determined, using the same elemental analyzer, on peat samples pre-dried at 420 °C for 12 h. In this case, urea was used as standard. Oxygen content was calculated by difference: $O\% = 100 - (C + H + N + S)\%$. All samples were analyzed in triplicate, and obtained data corrected for ash and moisture content. Ratios between elements (i.e., C/N, C/H and O/C) have been determined as atomic ratios, considering as C concentration those of the TOC.

2.3.4. Fourier transform infrared (FT-IR) spectroscopy

The FT-IR spectra of peat samples were acquired in transmittance mode using a Thermo Nicolet Nexus FT-IR Spectrophotometer equipped with Nicolet Omnic 6.0 software. Potassium bromide pellets were obtained by pressing, under vacuum, a homogenized mixture of 400 mg of infrared grade KBr and 1 mg of sample (d.w.). Spectra were recorded under a N_2 atmosphere in the range 4000–400 cm^{-1}, with a 2 cm^{-1} resolution and with 64 scans for each acquisition.

2.3.5. Molecular fluorescence

Fluorescence spectra were recorded on aqueous solutions of peat samples. In particular, 2 mg of sample (d.w.) were solubilised in few ml of NaOH (0.5 M) diluted with MilliQ water, at a concentration of 100 $mg l^{-1}$, equilibrated overnight at room temperature, and adjusted to pH 8 with 0.05 M NaOH. The suspensions were then filtered through 0.45 μm GF/C filters (modified from Zsolnay, 2003). Fluorescence spectra were recorded on each sample using a Perkin–Elmer (Norwalk, CT) LS-55 luminescence spectrophotometer, equipped with FL WinLab software (version 4.00.03). All spectra were recorded using the same instrumental conditions: emission and excitation slits were set at a 5 nm band width, and a scan speed of 500 nm min^{-1} was selected for both monochromators. Fluorescence spectra were electronically corrected for instrumental response, and both the sensitivity and stability of the instrument were previously measured using the Raman band signal intensity. Total luminescence spectra, in the form of excitation–emission matrix (EEM, contour maps), were recorded over the emission wavelength range from 300 to 600 nm, increasing sequentially by 5 nm step the excitation wavelength. The EEM plots were generated as contour maps from fluorescence data by using the Surfer 8.01 software (Golden Software Inc., 2002).

Positions and relative fluorescence intensity (RFI) values of individual fluorescent peaks were determined to gain information on changes in the composition of the peat extracts following the smouldering fire. Preliminary experiments carried out on samples with higher organic C concentration showed no changes due to inner filter effects and/or quenching phenomena.

2.3.6. UV–Vis spectroscopy

UV–Vis analyses were conducted using a PerkinElmer model Lambda 15 spectrophotometer. The molar absorptivity (or molar extinction coefficient) at 280 nm (ε_{280}) (l mole OC^{-1} cm^{-1}), i.e., the region where the $\pi \rightarrow \pi^*$ electron transitions occur for a number of aromatic substances (Chin et al., 1994), was recorded for each sample. Specific UV absorbance at 254 nm ($SUVA_{254}$) (l mg OC^{-1} m^{-1}) was calculated by normalizing the absorbance at this wavelength by the concentration in organic C of the

corresponding sample (Weishaar et al., 2003). All measurements were carried out a solution obtained by dissolving 0.15 g of each sample in 100 ml of aqueous NaOH (0.5 M), and than diluting again using a ratio 1:3 (v:v).

2.3.7. Statistical analyses

Statistical correlation and analysis of variance (ANOVA) were performed using the Statistica Version 9.1 software (StatSoft Inc., 2010). Significant differences were calculated on the basis of the Tukey's test, considering a significance level of $p < 0.05$.

3. RESULTS AND DISCUSSION

3.1. Depth of burn

The depth of burn is the vertical distance from the original sample surface to the location where the fire extinguished itself (Fig. 1a). Our laboratory tests exclude the effects of wind and rain, therefore the reasons why a smouldering front extinguishes at a particular location in a column sample is related to the controlling mechanisms of smouldering combustion (Rein, 2013). These controlling mechanisms are oxygen supply and heat transfer (Ohlemiller, 1985; Frandsen, 1987; Rein, 2013). Extinguishing is primarily due to the progressive reduction as the ash layer, and therefore the airflow resistance across it, builds up with depth. Due to this decrease of oxygen diffusion into the front, lower depths of burn are expected for weaker fires. For example, in samples of high MC, water evaporation is a substantial heat loss that causes extinction at shorter depths. Consequently, the depth of burn in these experiments represents a proxy for the general flammability of a peat column.

The experimental results show that the depth of burn decreases with MC. In the 50% MC peat column, the fire spread downwards from the top to the very bottom (21 cm depth of burn), whereas in the 100% MC it spread to a depth of 17 cm, leaving 9 cm of ash and char residues. The smouldering fire did not spread beyond the igniter region (top 7 cm) in the wettest peat column (200% MC), but the peat next to and on top of the igniter were affected by the fire due to nearby contact with the strong heat source. As the igniter was buried 5 cm into the column, the depth of burn for the 200% MC sample was 7 cm, just 2 cm deeper than the igniter.

We report in this work three MC experiments, but a total of six experiments were conducted at different values of MC ranging from 0% (oven-dry) to 200% to study the variability of the depth of burn. These included repeats of the 50%, 100% and 200% MC experiments. A linear and negative dependence between MC and depth of burn was obtained ($R^2 = 0.832$, $p = 0.011$), i.e., the higher the MC, the shorter the depth of burn.

3.2. Physical and chemical changes in smouldering peat

The fresh *Sphagnum* peat employed for the preparation of column tests was also used as control (FP). The main physical and chemical features of this *Sphagnum* peat are reported in Table 1 and they closely resemble those of the upper layers of ombrotrophic bogs (e.g., Cocozza et al., 2003; Zaccone et al., 2007).

In the following discussions, we define the depth from the front as the vertical distance into the residue starting from the position of the free surface after the test (Fig. 1). The results show that, when a smouldering front was established, it led to substantial changes for all the studied parameters with respect to the FP. These changes depend on both the initial MC and the depth of the sample, measured from where the front extinguished itself. Generally speaking, these variations were observed to be more significant in the layers closer the extinguished front, and occurred through the entire remaining profile in the 50% MC series, and within a depth of 8 cm in the 100% MC series. No relevant differences were observed for most of the studied parameters in the 200% MC, because the smouldering front did not propagate. In detail, comparing the burnt remains in the 50% and 100% MC series with the FP (Fig. 2a,b), an increase of the ash content, pH, EC, IC, TC, total N (TN) and of the C/H ratio was observed, whilst the C/N ratio was observed to decrease.

The significant increase of ash in soils following fires is well known since the beginning of agriculture and forestry (Pyne, 2001), as it leads to an enhancement of the available elements content (mainly in a water-soluble form) which, in turn, causes a raise in soil pH and EC. This phenomenon has been frequently observed in several other soils (e.g., grasslands, forests) after a (flaming) fire, although to a varying extent (Raison, 1979 and referene therein; González-Pérez et al., 2004 and reference therein), and has been generally associated with an increase in exchangeable cations (Viro, 1974; Raison, 1979), to the loss of OH groups resulting from the denaturing of the clay minerals, as well as to the formation of oxides of elements derived from disruption of the carbonates (Giovannini et al., 1990). However, these explanations do not justify the extent of enhanced pH observed in our laboratory experiments (i.e., from 3.9 ± 0.2 in FP to 8.0 ± 0.2 in the 50% MC series), considering that the mineral content in our peat is very

Table 1
Main physical and chemical features (avg. ± st. dev.; $n = 3$) of the *Sphagnum* peat used as control (FP). Elemental content is reported on dry, ash-free basis.

pH	EC (mS cm^{-1})	C (%)	H (%)	N (%)	S (%)	O (%)	C/N	C/H	O/C	Ash (%)
3.9 ± 0.2	0.20 ± 0.03	52.63 ± 0.36[†]	5.91 ± 0.01	1.31 ± 0.05	0.19 ± 0.06	39.97[‡]	46.6[§]	0.74[§]	0.67[§]	3.39 ± 0.18

[†] Of which inorganic C (%) = 0.41 ± 0.01.
[‡] Determined by difference [100 − (C + H + N + S)%].
[§] Determined as atomic ratio.

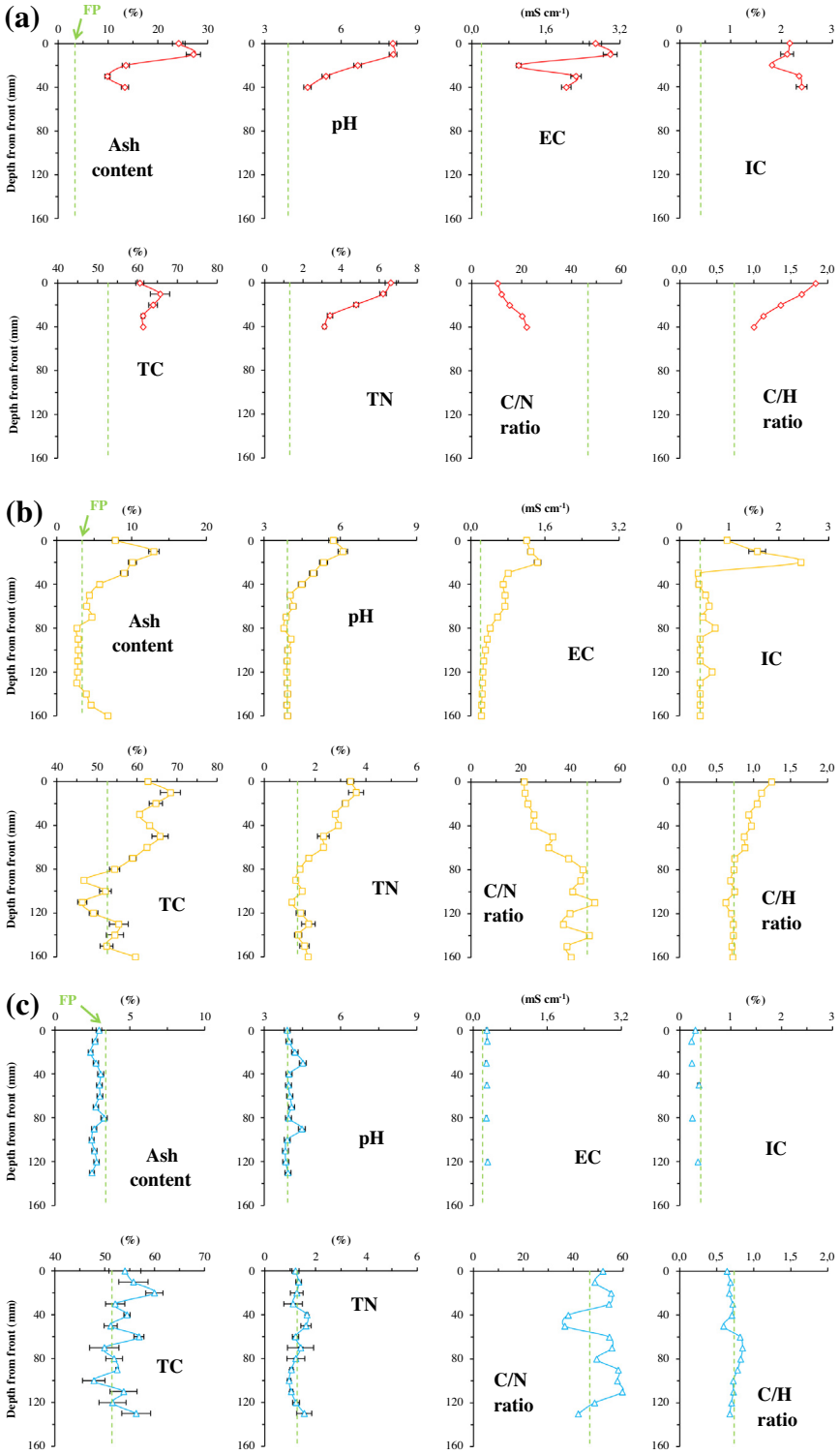

Fig. 2. Evolution of some physical and chemical features of the organic matter throughout the peat columns. The figure shows the variation of ash content, pH, EC, inorganic C, total C and N, C/N and C/H atomic ratios in the (a) 50% MC series; (b) 100% MC series; (c) 200% MC series (data only down a depth of 13 cm of depth have been plotted, as no significant variation was observed). Error bars represent standard deviations of the means ($n = 3$). The broken green line represents the average value of each parameter in the control (FP), i.e., in the peat column before the smouldering test. (For interpretation of the references to colour in this figure legend, the reader is referred to the web version of this article.)

low (i.e., 3.4 ± 0.2 in FP). Therefore, we suggest that, in *Sphagnum* dominated peatlands (e.g., bogs), the increase in pH is manly due to the decrease of acidic functional groups (e.g., carboxylic) in peat OM and the consequent release of CO and CO_2 to the atmosphere. At the same time, part of these gases could be re-dissolved in the water phase, thus promoting the formation and accumulation of ash rich in oxides and carbonates of basic ions (e.g., Ca, Mg). This is consistent with the increase of IC in our burnt peat samples (avg. values: 2.16 ± 0.23% and 0.86 ± 0.65% in 50% MC and 100% MC series, respectively) when compared with FP (0.41 ± 0.01%).

Both series show a general increase of TC and TN concentration in the burnt peat remains. In particular, TC reaches maximum values of 65.7 ± 2.4% and 68.3 ± 2.5% in the 50% and 100% MC series, respectively, *vs.* 52.6 ± 0.4% in the FP. In detail, TC was maximum 1.2 and 1.3 times higher in the 50% MC profile and the first 8 cm of the 100% MC series, respectively, when compared to the FP. A similar trend was observed for TN, showing maximum values of 6.60 ± 0.29% and 3.61 ± 0.28%, respectively, *vs.* 1.31 ± 0.05% in the FP. In detail, TN was from 2.4 to 5.1 times higher in the 50% MC profile, and from 1.3 to 2.8 higher in the first 8 cm of the 100% MC series, than in the FP. As peak temperatures reached during smouldering are too low (<450 °C) to disassociate atmospheric N_2, the N found in the fire residue is expected to come from N originally present in the peat, and not from atmospheric N.

The higher relative increase of TN compared to TC resulted in the decrease of the C/N ratio at a certain depth below where the fire front extinguished itself. That suggests the incorporation of, and the relative enrichment in, N during charring and highlights the importance of "black N" as an integral part of the resulting material. These data are in agreement with those reported by Knicker (2010) who hypothesized that N enrichment may result from the low thermal stability of the main plant constituent (i.e., cellulose), thus leading to a preferential loss of C, O and H, and to a relatively enrichment of peptide derived N compounds. Moreover, several authors have reported the formation of N-containing pyrogenic structures including pyrrole/indole-type N, pyridine N, pyrroline, and pyrrolidine as a consequence of vegetation fires (Knicker et al., 2008) and laboratory thermal oxidation of sapric peat (Almendros et al., 2003). Finally, the significantly higher C/H ratios found in the burnt peat samples from the 50% and 100% MC series indicates an increase of the aromatic degree with respect to the FP. Besides TC and TN, both 50% and 100% MC series show also an increase of total S concentration, ranging from 0.75 ± 0.17% to 1.34 ± 0.46% (0.95 ± 0.23, average value) and from 0.18 ± 0.03% to 0.45 ± 0.10% (0.30 ± 0.10, average value), respectively (data not shown), *vs.* 0.19 ± 0.06% in the FP (Table 1).

In the 200% MC, the only significant variation observed can be ascribed to the total organic C content and, as a consequence, of the C/N ratio (Fig. 2c), probably due to the dissolution and migration of the more labile OM, favoured by the extracting power of hot water produced by heat from the igniter.

A negative correlation in both 50% MC ($R^2 = 0.990$, $p < 0.01$) and 100% MC ($R^2 = 0.886$, $p < 0.0001$) series can be observed when plotting together the C/N and the C/H atomic ratios (Fig. 3a and Table 2). This indicates that the more aromatic the burnt peat is (higher C/H ratio), the more N is incorporated in the pyrogenic char (lower C/N ratio). Furthermore, plotting together the H/C and the O/C atomic ratios (Fig. 3b) in a van Krevelen diagram (van Krevelen, 1950), it is possible to observe that samples resulting from the smouldering fire in the 50% MC show a higher aromaticity (lower H/C ratio) and a lower polarity (lower O/C ratio) when compared with 100% and 200% MC series and the FP. At the same time, in both the 50% and 100% MC series, this phenomenon is more evident for the samples closer to the fire front, while it tends to disappear with depth.

3.3. Spectroscopic features of smouldering peat

3.3.1. FT-IR

The FT-IR spectrum of the *Sphagnum* peat used as control (FP) is characterized by a number of absorption bands exhibiting variable relative intensities, accordingly to the presence of cellulosic, hemi-cellulosic, ligno-cellulosic, lignin-derived structures and other plant by-products (Cocozza et al., 2003; Zaccone et al., 2007, 2008, 2011b). The main absorption bands observed are reported in Table 3.

As a consequence of the smouldering phenomena, FT-IR spectra of burnt peat samples feature a quite different shape with depth (i.e., with the increasing of the distance from the front), thus suggesting considerable variations of the molecular composition and the chemical structures of the peat remains throughout the profile and compared to the FP. In general, FT-IR spectra of the 50% and 100% MC samples (Fig. 4a, b) show that the aliphatic structures and the oxygen-containing functional groups (e.g., carboxyl and hydroxyl) are easily removed in the first layers following smouldering combustion, whereas aromatic moieties tend to increase. No relevant differences have been observed along the profile in 200% MC series (Fig. 4c). In detail, the main variations in absorption bands observed in the smouldered peat with respect to the FP are related to: (1) a general increase in the aromatic/aliphatic ratio, as underlined by a lower absorption intensity at *ca.* 2920–2850 cm^{-1} (aliphatic C-H stretching) and a simultaneous relative increase in absorption intensity at 1615–1625 cm^{-1} (mainly aromatic C=C stretching); (2) a general decreasing/disappearance of the peak at *ca.* 1700 cm^{-1} (C=O stretching of carbonyl and carboxyl groups); (3) the disappearance of the peak at 1063 cm^{-1}, ascribed to C–O stretching of polysaccharide or polysaccharide-like substances, and the simultaneous appearance of two peaks around 1110–1115 cm^{-1} and 1155–1160 cm^{-1}, probably ascribed to the increase of mineral impurities and/or the occurrence of S functional groups (e.g., C=S, S=O).

The differences reported above are more significant in the upper layers of the residual columns, and can be observed throughout the whole profile in the 50% MC series, and the first 8 cm of depth in the 100% MC series. This

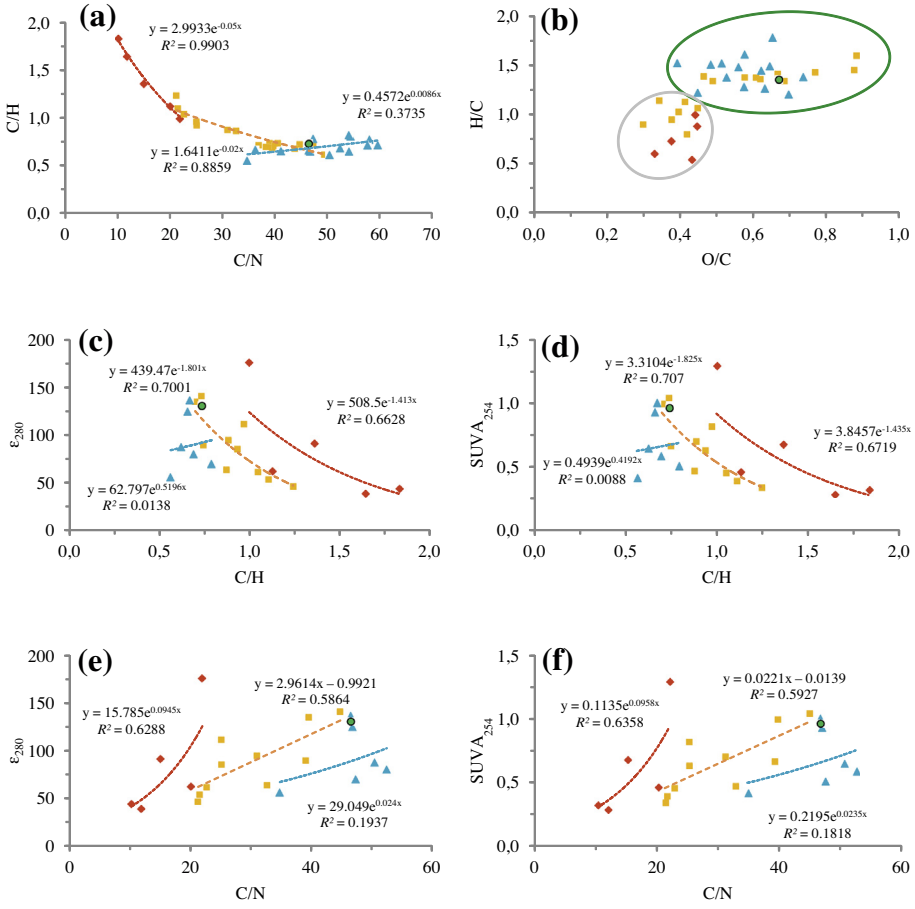

Fig. 3. Relationships between atomic ratios and spectroscopic parameters. Relationships between (a) C/N *vs.* C/H atomic ratio, (b) O/C *vs.* H/C atomic ratio [according to van Krevelen (1993), samples in the green circle show atomic ratios typical of peat, whereas samples in the grey circle are more similar to lignite], (c) C/H atomic ratio *vs.* ε_{280}, (d) C/H atomic ratio *vs.* $SUVA_{254}$, (e) C/N atomic ratio *vs.* ε_{280}, and (f) C/N atomic ratio *vs.* $SUVA_{254}$ [FP (●), 50% MC series (◆), 100% MC series (■), 200% MC series (▲)]. Statistical details are reported in Table 2.

Table 2
Statistical correlations. Significant correlations ($p < 0.05$) are reported in bold.

	C/H	C/N	O/C	ε_{280}	$SUVA_{254}$
(a) 50% MC series					
C/H					
C/N	$\mathbf{p = 0.0016}$ ($n = 5$)				
O/C	$p = 0.4536$ ($n = 5$)	$p = 0.3377$ ($n = 5$)			
ε_{280}	$p = 0.1321$ ($n = 5$)	$p = 0.1359$ ($n = 5$)	$p = 0.5060$ ($n = 5$)		
$SUVA_{254}$	$p = 0.1284$ ($n = 5$)	$p = 0.1330$ ($n = 5$)	$p = 0.3249$ ($n = 5$)	$\mathbf{p = 0.0000}$ ($n = 5$)	
(b) 100% MC series					
C/H					
C/N	$\mathbf{p = 0.0000}$ ($n = 17$)				
O/C	$\mathbf{p = 0.0004}$ ($n = 17$)	$\mathbf{p = 0.0001}$ ($n = 17$)			
ε_{280}	$\mathbf{p = 0.0052}$ ($n = 10$)	$\mathbf{p = 0.0098}$ ($n = 10$)	$p = 0.0049$ ($n = 10$)		
$SUVA_{254}$	$\mathbf{p = 0.0048}$ ($n = 10$)	$\mathbf{p = 0.0092}$ ($n = 10$)	$\mathbf{p = 0.0048}$ ($n = 10$)	$\mathbf{p = 0.0000}$ ($n = 10$)	
(c) 200% MC series					
C/H					
C/N	$\mathbf{p = 0.0248}$ ($n = 14$)				
O/C	$p = 0.7406$ ($n = 14$)	$p = 0.9204$ ($n = 14$)			
ε_{280}	$p = 0.8980$ ($n = 6$)	$p = 0.5172$ ($n = 6$)	$p = 0.3965$ ($n = 6$)		
$SUVA_{254}$	$p = 0.9245$ ($n = 6$)	$p = 0.5306$ ($n = 6$)	$p = 0.3771$ ($n = 6$)	$\mathbf{p = 0.0000}$ ($n = 6$)	

Table 3
Major IR adsorption bands and corresponding assignments.

Wavenumbers (cm^{-1})		Assignments
ca. 3440	b	O–H stretching of hydrogen bonded O–H groups
2922, 2853	p	Asymmetric stretching of aliphatic C–H
ca. 1700	p	C=O stretching of carbonyl functions, particularly aldehydes, ketones, and carboxyl groups
ca. 1630	b	Aromatic C=C vibrations and COO– symmetric stretching
1515	p	Aromatic skeletal vibrations, to conjugated C=N systems and amino functionalities
1380	p	O–H deformations of phenolic and aliphatic groups
1263	p	C–O stretching of ethers and/or carboxyl groups
1157	p	O–H stretching of alcoholic groups
ca. 1065	b	C–O stretching of polysaccharide or polysaccharide-like substances and Si–O stretching of mineral impurities

b = band; p = peak.

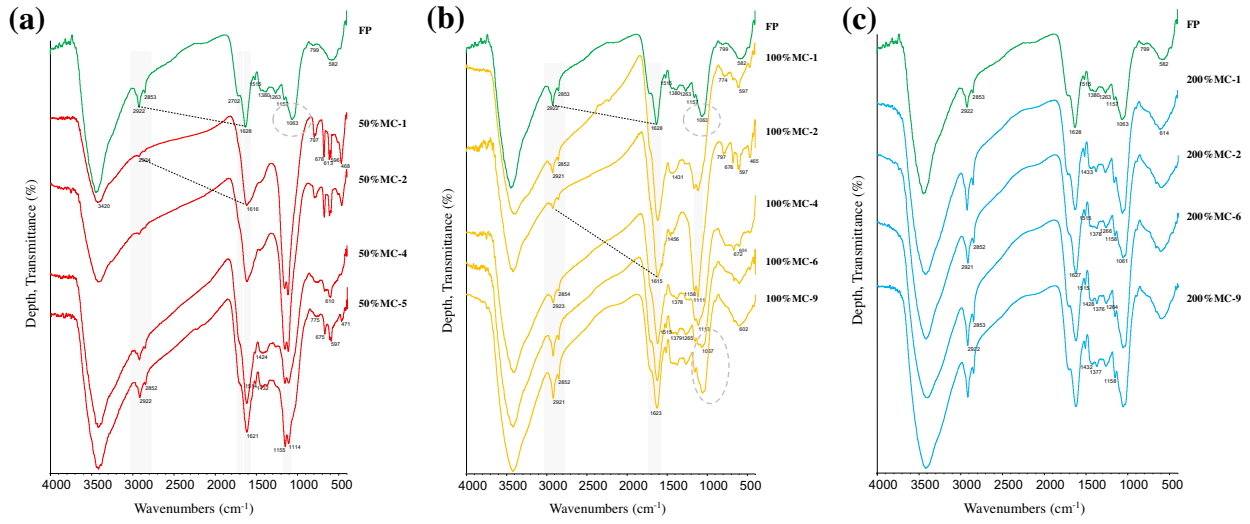

Fig. 4. FT-IR spectra of representative peat samples: (a) 50% MC series; (b) 100% MC series; (c) 200% MC series. The FT-IR spectrum of the original, undisturbed peat sample (control, FP) is reported in green. Major IR adsorption bands and corresponding assignments are reported in Table 3. Main changes in absorption bands are underlined in grey; in particular, dashed grey circles in Fig. 3a and b highlight the occurrence/disappearance of the peak generally ascribed to C–O stretching of polysaccharide and polysaccharide-like substances. Different numbers at the end of the sample name indicate a different depth (in cm). (For interpretation of the references to colour in this figure legend, the reader is referred to the web version of this article.)

finding is in full agreement with changes observed considering both physical (i.e., ash) and chemical parameters (i.e., C/H and O/C atomic ratios, changes in S concentration).

3.3.2. Molecular fluorescence and UV–Vis

Both molecular fluorescence and UV–Vis spectroscopy revealed several differences between the smouldered samples and the FP, as well as among different MC series. Again, variations were more significant in the upper layers of the columns, and regarded the whole profile in the 50% MC series, and the first 8 cm of depth in the 100% MC series. No relevant differences have been observed along the 200% MC profile.

In particular, Fig. 5 clearly shows:

(a) An increase of the RFI of the main fluorophore in burnt peat samples compared to the FP, probably due to the formation of simpler and aromatic organic molecules (Senesi, 1990). Then, the RFI generally decreases with depth.

(b) A shift of the main fluorophore to lower excitation/emission wavelength pairs (EEWP) (e.g., $320_{exc}/415_{em}$ and $335_{exc}/445_{em}$ in the 50% MC-1 and 100% MC-2, respectively) with respect to the FP ($345_{exc}/450_{em}$). Observed shifts are function of the depth from the front (i.e., largest shifts occurred in correspondence of short distances) and probably mirror the fire severity, being the latter one function of the MC (e.g., 50% *vs.* 100% MC).

(c) The occurrence of a secondary fluorophore, generally located at EEWP of $250_{exc}/420–450_{em}$, that could be probably ascribed to the formation of N-containing pyrogenic structures (e.g., pyrrole-type N; Knicker et al., 2005).

UV–Vis spectroscopy confirmed the findings of the molecular fluorescence. First of all, it is to notice that ε_{280} and $SUVA_{254}$, both positively related with the aromaticity and the molecular complexity, are significantly correlated to each other ($R^2 = 0.997$, $p < 0.0001$, $n = 21$). In particu-

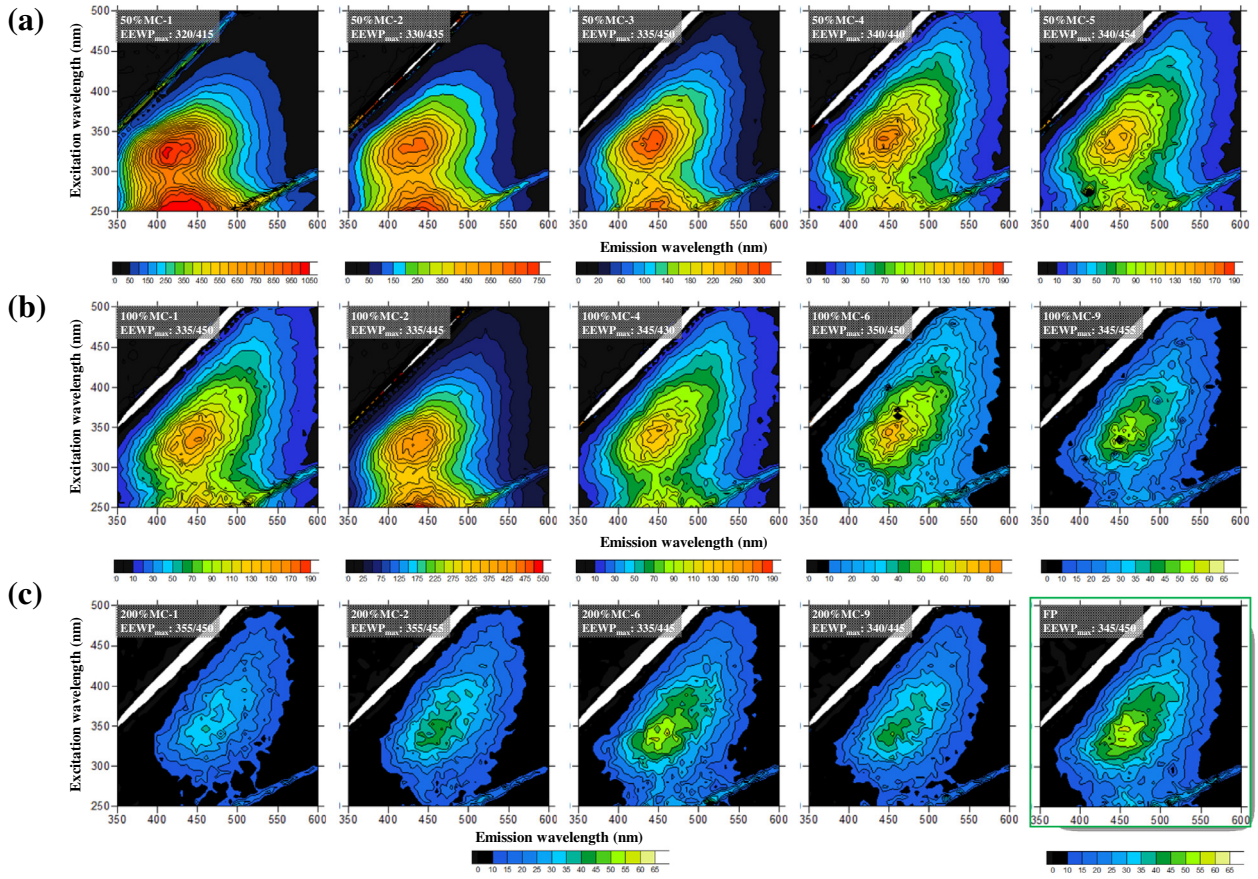

Fig. 5. Total luminescence spectra in the form of excitation–emission matrices (EEM) of representative peat samples: (a) 50% MC series; (b) 100% MC series; (c) 200% MC series. The EEM matrix of the original, undisturbed peat sample (control, FP) is shown in the bottom, right corner. Excitation/emission wavelength pairs at the maximum fluorescence intensity ($EEWP_{max}$) are also reported. Relative fluorescence intensity (RFI) is expressed in arbitrary units. Different numbers at the end of the sample name indicate a different depth (in cm).

lar, ε_{280} values ranged between 39.5 and 175.9 l mole OC^{-1} cm^{-1} in the 50% MC, and between 47.2 and 135.3 l mole OC^{-1} cm^{-1} in the 100% MC (*vs.* 131.0 in FP), while $SUVA_{254}$ values ranged between 0.3 and 1.3 l mg OC^{-1} m^{-1} in the 50% MC, and between 0.4 and 1.0 l mg OC^{-1} m^{-1} in the 100% MC (*vs.* 1.0 in FP). Both spectroscopic indices showed values increasing with depth.

The relationships between ε_{280} and C/H, and between $SUVA_{254}$ and C/H (Fig. 3c, d and Table 2), are strongly dependent on the chemical processes occurring and the peak temperature which decreases with depth (Fig. 1c, d). This is particularly evident for the 50% and 100% MC series. The low ε_{280} and $SUVA_{254}$ values observed for the peat extract from the samples closer to the fire front are possibly associated to the occurrence of small and simple aromatic molecules showing very discrete fluorophores (Fig. 5), i.e., a high fluorescence efficiency (Senesi, 1990). This result matches with the high C/H and low O/C values observed for the corresponding solid samples, possibly ascribed to highly condensed aromatic moieties deriving from the pyrolysis of the organic structures. With the decreasing peak temperature as depth increases, the pyrolysis effect of aromatic condensation of the solid phase of peat is probably reduced as indicated by the decrease of the C/H ratio and increase of O/C ratio, and by the progressive increase of the ε_{280} and $SUVA_{254}$ until the maximum depth. There, in fact, the soluble fraction of the peat samples is likely characterized by a very wide molecular diversity and, consequently, higher molecular absorption with a resulting decrease of the fluorescence (or quantum) efficiency of the peat extracts (Fig. 5).

As a consequence of the inverse relationship between the C/H and the C/N ratios (Fig. 3a), peat samples showing a lower C/N ratio (i.e., higher N content) seem to correspond, in the peat extracts, to more simple organic molecules with very discrete fluorophores (low ε_{280} and $SUVA_{254}$) (Fig. 3e, f). Therefore, trends shown in Fig. 3(c–f) describe the inverse relationships between the organic molecules in the liquid phase (i.e., the more soluble ones), whose physical expression (e.g., molecular conformation and shape, aggregation state) is a function of the surrounding chemical conditions (Senesi, 1990), and the solid, bulk OM, whose structure and complexity are a function of the pyrolytic gradient.

This finding is also extremely important as underscores that data obtained on the peat extracts (or peat liquid phase) using UV–Vis and molecular fluorescence could not always be sufficient to correctly understand and explain

complex phenomena. As they could be in complete agreement or just represent the "negative", data obtained on peat extracts need to be coupled to analyses carried out on the corresponding solid phase.

4. POSSIBLE IMPLICATIONS FOR PALAEOFLORAL AND PALAEOCLIMATIC RECONSTRUCTIONS

The findings reported in this study suggest the possibility that similar chemical and physical signatures detected previously throughout peat cores might have been wrongly ascribed to past environmental changes (e.g., climatic, floral, hydrological variations). The possibility that such changes may be the result of smouldering fires has not been considered before. For example, peaks in ash content, such as those observed in our study (i.e., *ca.* 27% and 13% in the 50% MC and 100% MC series, respectively, *vs. ca.* 3% in the FP), have in the past been ascribed to an increase of either dust depositions or mineralization processes, typically linked to climatic changes (Zaccone et al., 2012 and reference therein). Similarly, large variations in pH values (i.e., from <4 in the FP to >8 and >5 in the 50% MC and 100% MC series, respectively) and EC (that was 5–15 and 2–8 times higher in the 50% MC and 100% MC series, respectively, than the FP) following a smouldering fire could have been wrongly ascribed to a transition from ombrotrophic-to-minerotrophic conditions or *vice versa* (Shotyk, 1988), depending on the depth of the smouldered horizon. And the bog-to-fen or fen-to-bog transition reflects, in turn, environmental changes, including climatic, floral and hydrological changes.

Likewise, variations in C/N ratio, such as those observed in our experiments, have been often suggested to reflect, although with some limitations, changes in the vegetation composition, in the humification degree of peat, or both (Kuhry and Vitt, 1996; Hornibrook et al., 2000; Zaccone et al., 2008, 2011a, 2012), that, in turn, might reflect variations either in the trophic status of the peatland or in the depth of the water table, both of them induced mainly by climatic changes (Charman, 2002).

We believe that our data provide an important additional contribution towards a more accurate assessment of palaeoenvironmental conditions, especially when the fossil record of palaeofires in the form of charcoal (which does not consider smouldering fires) is absent or if possible biomarkers of the fire history (e.g., N-containing pyrogenic structures, levoglucosan) are not well preserved. For example, Pitkänen et al. (2001), describing the natural fire regime as obtained analyzing peat strata from Finland, reported some lack of agreement between dendrochronological estimates and number of charcoal layers, as well as little evidence of fires during a particularly dry period (5290–5920 cal. yr BP). Moreover, the utilization of biomarkers of fire events (e.g., N-containing pyrogenic structures, levoglucosan) has to be taken with caution, as they might show a low stability in dry, oxic, less acidic post-fire environments (Knicker et al., 2013) like a peatland following a smouldering fire. Levoglucosan could be completely degraded or reworked by microorganisms (Kitamura et al., 1991; Xie et al., 2006; Knicker et al., 2013), thus leading to an underestimation of palaeofires. Hydrolysis over millennial time periods also needs to be evaluated, according to Elias et al. (2001). At the same time, several authors demonstrated the occurrence of levoglucosan almost exclusively in low temperature char (i.e., <350 °C; Kuo et al., 2008; Knicker et al., 2013); thus, this marker could be a good candidate to distinguish, in some cases, between "recent" flaming (higher temperature) *vs.* smouldering (lower temperature) fires occurring in peat.

Finally, our results highlight that smouldering fires have probably been overlooked as the cause of both physical and chemical variations observed in peat cores, and that smouldering fires should be considered in interpretations of palaeoenvironmental changes.

5. CONCLUSIONS

Measurements carried out on the peat columns after the smouldering fire show a general variation of the physical and chemical properties across the interface between the burnt residue and the undisturbed peat. In particular, strong increases of pH, EC, ash content, TN, and C/H ratio, and a strong decrease in C/N and O/C ratios were observed in the peat columns of 50% and 100% MC. The depth over which the chemical markers vary extends the whole residual column in 50% MC, and 8 cm deep in 100% MC. No relevant variation of any of the considered parameters is observed in 200% MC peat column.

The results of this study show that smouldering fires could occur when peatlands are in quite dry conditions. This is particularly important as warmer temperatures at high latitudes are already resulting in unprecedented permafrost thaw, leaving large organic C pools exposed to fires for the first time in millennia. Following smouldering, there is a higher production of aromatic and condensed molecules a few centimetres below the fire front, as suggested by the variation in C/H and O/C values and by FT-IR and fluorescence spectra. Moreover, the relative enrichment in N observed suggests its incorporation into pyrogenic-OM and underlines the importance of "black N" as an integral part of the char.

Consequently, smouldering events should be considered in palaeoenvironmental reconstructions from ombrotrophic peat cores. This is particularly important when interpreting, for example, peaks in ash content or variations of the C/N ratio in Quaternary peat cores, as these could be as much related to palaeofires as to other environmental perturbations (e.g., dust depositions, OM mineralization, changes in either vegetation or humification degree).

Further research is required to consider physical and chemical signatures that may allow reconstruction of smouldering fires from peat cores or other older organic deposits, in absence of fossil charcoals or specific recalcitrant pyrogenic biomarkers.

ACKNOWLEDGEMENTS

C.Z. acknowledges the Italian Ministry for University and Research (MIUR) for financing part of the present research (PRIN program 2009; 2009NBHPWR – Project title: "Chemical and

biomolecular indicators for reconstructing environmental changes in natural archives"). G.R. acknowledges funding from the Royal Academy of Engineering, the Leverhulme Trust and EPSRC. The authors would like to acknowledge Abubakar Alkatib for his help in conducting the laboratory fire tests, and Prof. William Shotyk, University of Alberta, Canada, for helpfull discussions. The authors are also indebted to anonymous referees for their valuable comments and suggestions on the previous version of the manuscript.

REFERENCES

Aaby B. (1976) Cyclic climatic variations in climate over the past 5,500 yr reflected in raised bogs. *Nature* **263**, 281–284.

Alexis M. A., Rasse D. P., Knicker H., Anquetil C. and Rumpel C. (2012) Evolution of soil organic matter after prescribed fire: a 20-year chronosequence. *Geoderma* **189–190**, 98–107.

Almendros G., Knicker H. and González-Vila J. F. (2003) Rearrangement of carbon and nitrogen forms in peat after progressive thermal oxidation as determined by solid state ^{13}C and ^{15}N NMR spectroscopy. *Org. Geochem.* **34**, 1559–1568.

Beck P. S. A., Goetz S. J., Mack M. C., Alexander H. D., Jin Y., Randerson J. T. and Loranty M. M. (2011) The impacts and implications of an intensifying fire regime on Alaskan boreal forest composition and albedo. *Global Change Biol.* **17**, 2853–2866.

Belcher C., Yearsley J., Hadden R., McElwain J. and Rein G. (2010) Baseline intrinsic flammability of Earth's ecosystems estimated from paleoatmospheric oxygen over the past 350 million years. *Proc. Natl. Acad. Sci. USA* **107**, 22448–22453.

Benscoter B. W., Thompson D. K., Waddington J. M., Flannigan M. D., Wotton B. M., De Groot W. J. and Turetsky M. R. (2011) Interactive effects of vegetation, soil moisture and bulk density on depth of burning of thick organic soils. *Int. J. Wildland Fire* **20**, 418–429.

Certini G. (2005) Effects of fire on properties of forest solid: a review. *Oecologia* **143**, 1–10.

Charman D. (2002) *Peatlands and Environmental Change*. Wiley and Sons Ltd., Chichester, p. 301.

Chin Y.-P., Alken G. and O'Loughlin E. (1994) Molecular weight, polydispersity, and spectroscopic properties of aquatic humic substances. *Environ. Sci. Technol.* **28**, 1853–1858.

Cocozza C., D'Orazio V., Miano T. M. and Shotyk W. (2003) Characterization of solid and aqueous phases of a peat bog profile using molecular fluorescence spectroscopy, ESR and FT-IR, and comparison with physical properties. *Org. Geochem.* **34**, 49–60.

Elias V. O., Simoneit B. R. T., Cordeiro R. C. and Turcq B. (2001) Evaluating levoglucosan as an indicator of biomass burning in Carajás, Amazonia: a comparison to the charcoal record. *Geochim. Cosmochim. Acta* **65**, 267–272.

Field R. D., van der Werf G. R. and Shen S. S. P. (2009) Human amplification of drought-induced biomass burning in Indonesia since 1960. *Nat. Geosci.* **2**, 185–188.

Frandsen W. H. (1987) The influence of moisture and mineral soil on the combustion limits of smouldering forest duff. *Can. J. For. Res.* **17**, 1540–1544.

Frandsen W. H. (1997) Ignition probability of organic soils. *Can. J. For. Res.* **27**, 1471–1477.

Giovannini G., Lucchesi S. and Giachetti M. (1987) The natural evolution of a burned soil: a three-year investigation. *Soil Sci.* **143**, 220–226.

Giovannini G., Lucchesi S. and Giachetti M. (1990) Effect of heating on some chemical parameters related to soil fertility and plant growth. *Soil Sci.* **149**, 344–350.

González-Pérez J. A., González-Vila F. J., Almendros G. and Knicker H. (2004) The effect of fire on soil organic matter – a review. *Environ. Int.* **30**, 855–870.

Hadden R., Rein G. and Belcher C. (2013) Study of the competing chemical reactions in the initiation and spread of smouldering combustion in peat. *Proc. Combust. Inst.* **34**, 2547–2553.

Hornibrook E. R. C., Longstaffe F. J., Fyfe F. S. and Bloom Y. (2000) Carbon-isotope ratios and carbon, nitrogen and sulfur abundances in flora and soil organic matter from a temperate-zone bog and marsh. *Geochem. J.* **34**, 237–245.

Kitamura Y., Abe Y. and Yasui T. (1991) Metabolism of levoglucosan (1,6-anhydro-β-D-glucopyranose) in microorganisms. *Agric. Biol. Chem.* **55**, 515–521.

Klemetti V. and Keys D. (1983) Relationships between dry density, moisture content, and decomposition of some New Brunswick peats. In *Testing of Peats and Organic Soils* (ed. P. M. Jarrett). American Society for Testing and Materials, pp. 72–82.

Knicker H. (2010) "Black nitrogen" – an important fraction in determining the recalcitrance of charcoal. *Org. Geochem.* **41**, 947–950.

Knicker H., González-Vila F. J., Polvillo O., González J. A. and Almendros G. (2005) Fire induced transformation of C- and N-forms in different organic soil fractions from a Dystric Cambisol under a Mediterranean pine forest (Pinus pinaster). *Soil Biol. Biochem.* **37**, 701–718.

Knicker H., Hilscher A., de la Rosa J. M., González-Pérez J. A. and González-Vila F. J. (2013) Modification of biomarkers in pyrogenic organic matter during the initial phase of charcoal biodegradation in soils. *Geoderma* **197–198**, 43–50.

Knicker H., Hilscher A., González-Vila F. J. and Almendros G. (2008) A new conceptual model for the structural properties of char produced during vegetation fires. *Org. Geochem.* **39**, 935–939.

Kuhry P. and Vitt D. H. (1996) Fossil carbon/nitrogen ratios as a measure of peat decomposition. *Ecology* **77**, 271–275.

Kuo L.-J., Herbert B. E. and Louchouarn P. (2008) Can levoglucosan be used to characterize and quantify char/charcoal black carbon in environmental media?. *Org. Geochem.* **39** 1466–1478.

Langdon P. G., Brown A. G., Caseldine C. J., Blockley S. P. E. and Stuijts I. (2012) Regional climate change from peat stratigraphy for the mid- to late Holocene in central Ireland. *Quat. Int.* **268**, 145–155.

Mooney S. D. and Tinner W. (2011) The analysis of charcoal in peat and organic sediments. *Mires Peat* **7**, 1–18.

Moreno L., Jiménez M. E., Aguilera H., Jiménez P. and de la Losa A. (2011) The 2009 smouldering peat fire in Las Tablas de Daimiel National Park (Spain). *Fire Technol.* **47**, 519–538.

Ohlemiller T. J. (1985) Modeling of smoldering combustion propagation. *Prog. Energy Combust. Sci.* **11**, 277–310.

Page S. E., Siegert F., Rieley J. O., Boehm H. V., Jaya A. and Limin S. (2002) The amount of carbon released from peat and forest fires in Indonesia during 1997. *Nature* **420**, 61–65.

Pitkänen A., Tolonen K. and Jungner H. (2001) A basin-based approach to the long-term history of forest fires as determined from peat strata. *Holocene* **11**, 599–605.

Poto L., Gabrieli J., Crowhurst S. J., Appleby P. G., Ferretti P., Surian N., Cozzi G., Zaccone C., Turetta C., Pini R., Kehrwald N. and Barbante C. (2013) The first continuous Late Glacial – Holocene peat bog multi-proxy record from the Dolomites (NE Italian Alps). *Quat. Int.* **306**, 71–79.

Poulter B., Christensen, Jr., N. L. and Halpin P. N. (2006) Carbon emissions from a temperate peat fire and its relevance to interannual variability of trace atmospheric greenhouse gases. *J. Geophys. Res.* **111**, D06301.

Pyne S. J. (2001) *Fire: a Brief History. Weyerhauser Environmental Books, Cycle of Fire Series*. University of Washington Press, Seattle, USA, p. 204.

Raison R. J. (1979) Modifications of the soil environment by vegetation fires, with particular reference to nitrogen transformations: a review. *Plant Soil* **51**, 73–108.

Rein G. (2013) Smouldering fires and natural fuels, Chapter 2. In *Fire Phenomena in the Earth System – An Interdisciplinary Approach to Fire Science* (ed. C. Belcher). Wiley and Sons, pp. 15–33.

Rein G., Cleaver N., Ashton C., Pironi P. and Torero J. L. (2008) The severity of smouldering peat fires and damage to the forest soil. *Catena* **74**, 304–309.

Scott A. C. (2010) Charcoal recognition, taphonomy and uses in palaeoenvironmental analysis. *Palaeogeogr. Palaeoclimatol. Palaeoecol.* **291**, 11–39.

Senesi N. (1990) Molecular and quantitative aspects of the chemistry of fulvic acids and its interactions with metal ions and organic chemicals. Part II. The fluorescence spectroscopy approach. *Anal. Chim. Acta* **232**, 77–106.

Shotyk W. (1988) Review of the inorganic geochemistry of peats and peatland waters. *Earth-Sci. Rev.* **25**, 95–176.

Shotyk W., Krachler M., Martinez-Cortizas A., Cheburkin A. K. and Emons H. (2002) A peat bog record of natural, pre-anthropogenic enrichments of trace elements in atmospheric aerosols since 12 370 ^{14}C yr BP, and their variation with Holocene climate change. *Earth Planet. Sci. Lett.* **199**, 21–37.

Smith N. R., Kishchuk B. E. and Mohn W. W. (2008) Effects of wildfire and harvest disturbances on forest soil bacterial communities. *Appl. Environ. Microbiol.* **74**, 216–224.

Smith S. M., Newman S., Garrett P. B. and Leeds J. A. (2001) Differential effects of surface and peat fire on soil constituents in a degraded wetland of the northern Florida Everglades. *J. Environ. Qual.* **30**, 1998–2005.

Tareq S. M., Tanaka N. and Ohta K. (2004) Biomarker signature in tropical wetland: lignin phenol vegetation index (LPVI) and its implications for reconstructing the paleoenvironment. *Sci. Total Environ.* **324**, 91–103.

Tarnocai C., Canadell J. G., Schuur E. A. G., Kuhry P., Mazhitova G. and Zimov S. (2009) Soil organic carbon pools in the northern circumpolar permafrost region. *Global Biogeochem. Cycles* **23**, GB2023.

van Geel B. (1978) A palaeoecological study of holocene peat bog sections in Germany and The Netherlands, based on the analysis of pollen, spores and macro- and microscopic remains of fungi, algae, cormophytes and animals. *Rev. Palaeobot. Palynol.* **25**, 1–120.

van Krevelen D. W. (1950) Graphical–statistical method for the study of structure and reaction processes of coal. *Fuel* **29**, 269-84.

van Krevelen D. W. (1993) *Coal Typology, Physics, Chemistry, Constitution*, third ed. Elsevier, Amsterdam.

Villar M. C., Petrikova V., Díaz-Raviña M. and Carballas T. (2004) Changes in soil microbial biomass and aggregate stability following burning and soil rehabilitation. *Geoderma* **122**, 73–82.

Viro P. J. (1974) Effects of forest fires on soil. In *Fire and Ecosystems* (eds. C. E. Kozlowski and C. E. Ahlgren). Academic Press, New York, pp. 7–45.

Xie H., Zhuang X., Bai Z., Qi H. and Zhang H. (2006) Isolation of levoglucosan-assimilating microorganisms from soil and an investigation of their levoglucosan kinases. *World J. Microbiol. Biotechnol.* **22**, 887–892.

Watts A. C. (2013) Organic soil combustion in cypress swamps: moisture effects and landscape implications for carbon release. *For. Ecol. Manage.* **294**, 178–187.

Weishaar J. L., Aiken G. R., Bergamaschi B. A., Fram M. S., Fujii R. and Mopper K. (2003) Evaluation of specific ultraviolet absorbance as an indicator of the chemical composition and reactivity of dissolved organic carbon. *Environ. Sci. Technol.* **37**, 4702–4708.

Zaccone C., Casiello G., Longobardi F., Bragazza L., Sacco A. and Miano T. M. (2011a) Evaluating the 'conservative' behaviour of stable isotopic ratios (δ^{13}C, δ^{15}N, and δ^{18}O) in humic acids and their reliability as paleoenvironmental proxies along a peat sequence. *Chem. Geol.* **285**, 124–132.

Zaccone C., D'Orazio V., Shotyk W. and Miano T. M. (2009) Chemical and spectroscopic investigation of porewater and aqueous extracts of corresponding peat samples throughout a bog core (Jura Mountains, Switzerland). *J. Soils Sed.* **9**, 443–456.

Zaccone C., Miano T. M. and Shotyk W. (2007) Qualitative comparison between raw peat and related humic acids in an ombrotrophic bog profile. *Org. Geochem.* **38**, 151–160.

Zaccone C., Miano T. M. and Shotyk W. (2012) Interpreting the ash trend within ombrotrophic bog profiles: atmospheric dust depositions vs. mineralization processes. The Etang de la Gruère case study. *Plant Soil* **353**, 1–9.

Zaccone C., Said-Pullicino D., Gigliotti G. and Miano T. M. (2008) Diagenetic trends in the phenolic constituents of *Sphagnum*-dominated peat and its corresponding humic acid fraction. *Org. Geochem.* **39**, 830–838.

Zaccone C., Sanei H., Outridge P. M. and Miano T. M. (2011b) Studying the humification degree and evolution of peat down a Holocene bog profile (Inuvik, NW Canada): a petrological and chemical perspective. *Org. Geochem.* **42**, 399–408.

Zsolnay A. (2003) Dissolved organic matter: artefacts, definitions, and functions. *Geoderma* **113**, 187–209.

Associate editor: Peter Hernes